# Nuclear Magnetic Resonance Imaging of Transient Three-Dimensional Moisture Distribution in an Ear of Corn During Drying

HUAIPU SONG and J. BRUCE LITCHFIELD[1]

**ABSTRACT**

A three-dimensional Fourier transform method and a multislice two-dimensional Fourier transform method were used to obtain three-dimensional proton density images of an ear of corn. Two-dimensional, transient moisture profiles were obtained from the three-dimensional images. The moisture transfer and shrinkage of the sample were analyzed from the profiles. Mass transfer occurred in the $x$ and $z$ directions in individual kernels, but the mass transfer between kernels was negligible.

Cereal Chem. 67(6):580–584

Drying is an important process in the production of food products and in the preservation of foods and grains. The transient moisture profiles that occur during drying are important data for basic research about drying processes, modeling of transport and degradation phenomena, and development of process control schemes. But transient moisture profiles are difficult to measure accurately, especially in small food materials.

Moisture profiles in drying food materials have been obtained by various destructive methods. A peeling method was used by Andrieu and Stamatopoulos (1986). Layers of pasta were pressed together before drying. At different drying stages, pasta layers were peeled from each of the samples, and the moisture was measured. Moisture profiles were obtained from the average moisture content of each layer. Transient moisture profiles were also obtained by slicing partially dried frozen pasta at different drying stages and measuring the moisture content of the slices (Litchfield and Okos 1986). In these studies, errors were generated because of the moisture lost during measuring.

One-dimensional transient moisture profiles have been measured nondestructively during the drying of an ear of corn by two-dimensional Fourier transform (2-DFT) nuclear magnetic resonance (NMR) imaging (Song and Litchfield 1988). The profiles were determined from transverse proton density images, which were obtained during drying without disturbing the drying process. The proton density distribution was proportionally converted into moisture profile data for the corn. Moisture transfer and shrinkage information in the two-dimensional (2-D) plane were found from these results.

In a real drying process, however, moisture transfer occurs in three-dimensional (3-D) space. To obtain a thorough understanding of moisture transfer during drying and to evaluate drying models, accurate 3-D transient moisture images are needed. These data, however, have not been obtained until now.

NMR imaging (NMRI) has been widely applied in medical research and diagnostics for nondestructively measuring the density of active nuclei as a function of spatial coordinates. Several techniques have been used for obtaining 3-D images. The multislice (multiplanar) imaging method was proposed by Mansfield and Maudsley (1976). In multislice imaging, the 2-D slices are defined by selective excitation during the data acquisition. Each slice is excited in sequence during each imaging cycle. The first radio-frequency (RF) pulse excites and reads a spin echo from the sample in the first slice. The other slices are then tuned in and excited in sequence. A 3-D image is reconstructed by combining these slices. The major advantage of this method is its fast speed. All data can be collected at the same time for a single 2-DFT imaging experiment. The major disadvantage of this method is its poor resolution in the slice-selection direction, because the slice thickness is limited by the magnetic field gradient strength of the imaging system.

[1]Graduate Assistant and Assistant Professor, respectively, Agricultural Engineering Department, University of Illinois, Urbana, 61801.

The 3-D Fourier transform (3-DFT) imaging method is a planar technique that acquires the data from the whole volume of the sample at one time (Kumer et al 1975). A phase-encoding gradient is used in the slice-selection direction ($z$ direction) as in the 2-DFT method. Excitation occurs throughout the whole volume. Two phase-encoding gradients in the $x$ and $z$ directions are usually applied simultaneously. Data collection occurs during the subsequent application of the readout gradient in the $y$ direction. 3-D isotropic resolution is possible with this method. However, the method requires a relatively long acquisition time because of the larger number of imaging cycles required. Also, the image reconstruction process is rather long because the data from a 3-D imaging experiment must first be redimensioned as a 3-D array, and then the 3-DFT is performed on this array. The main advantage of the 3-DFT technique over the 2-D multislice technique is the former's ability to provide thin contiguous slices and the ability to obtain images in multiple display planes from a single acquisition (Stark and Bradley 1988).

Projection reconstruction is another technique used to obtain 3-D images (Lauterbur 1973). The image is reconstructed from a sufficient number of projections of the nuclear spin density contained in the sample. To obtain a projection of the 3-D spin density onto a straight line, a sufficiently strong magnetic field gradient is applied along the chosen direction. Nuclear spins in a plane perpendicular to this direction all contribute to resonance at the same frequency. One of the advantages of this method is that all volume elements are simultaneously excited, and the resulting transverse magnetization is observed during the entire available time. So this method yields a higher signal-to-noise ratio than the 3-DFT method with the same data acquisition time. However, this increases the volume of data acquired and thus takes longer than other methods for data processing.

The signal-to-noise ratio, resolution, and contrast of NMR images are directly controlled by sample characteristics such as nuclear density, the magnetic relaxation times, and the diffusion coefficient and by operational factors such as pulse sequence and sequence parameters. To interpret an image, the basic relationship between the signal intensity collected and these factors should be understood.

For the widely used Hahn spin-echo pulse sequence, which is expressed as 90°-$\tau$-180°-$\tau$ (Hahn 1950), where 90° and 180° represent 90 and 180° RF pulses and $\tau$ is a time constant, the NMR signal intensity ($S$) from a volume element, assuming a rectangular pulse profile, is:

$$S = N(H)\{1 - 2\exp[-(TR - TE/2)/T1] + \exp(-TR/T1)\} \times \exp(-TE/T2) \quad (1)$$

where $N(H)$ is the spin-density factor, $TR$ is the imaging cycle repetition time between pulse sequences, and $TE$ is echo time ($TE = 2\tau$), which consists of the time between the 90° RF pulse and the formation of the spin echo. $T1$ is the spin-lattice relaxation time, which is the time required for the sample to return to its original state by releasing the absorbed RF energy to the environment, and $T2$ is the spin-spin relaxation time, which is the rate at which the magnetic moments lose their directional coherence and reestablish their dephased orientations. By varying the two user-selectable delay times, $TE$ and $TR$, the spin-density images, which show only spin-density distribution, or $T1$-weighted and $T2$-weighted images, which highlight different components of the sample, can be obtained.

Molecular diffusion during the data acquisition period also affects the signal intensity. The effect of diffusion on the signal intensity for the spin-echo pulse sequence is as follows (Carr and Purcell 1954):

$$S \propto \exp(-\gamma^2 G^2 D \times TE \times \tau^2/3) \quad (2)$$

where $\gamma$ is the magnetogyric ratio, $G$ is the magnetic gradient strength, and $D$ is the diffusion coefficient.

Equation 1 describes how the NMR signal is affected by the sample characteristics $N(H)$, $T1$, and $T2$ and by the NMRI experimental parameters $TR$ and $TE$ when the diffusion effect is negligible. When the diffusion is significant, its effect on the NMR signal intensity can be evaluated according to the right side of expression 2. To study moisture transfer during drying, moisture distribution at different drying periods is required. Since moisture content is proportional to proton density, the proton-density images are required. According to equation 1 and expression 2, the effects of $TR$, $TE$, and diffusion on the signal intensity can be calculated, and pure proton-density images can be obtained.

The objectives of this study were to obtain a 3-D proton density image of an ear of corn and to measure 2-D moisture profiles during the drying of an ear of sweet corn.

## MATERIALS AND METHODS

An ear of fresh sweet corn was used for this study. The corn was stored at 4°C for one day before the drying tests. A 6-cm long section was cut from the whole ear of corn to be the sample. A spectroscopy imaging system 200-MHz, 330-mm instrument was used (Fig. 1). An imaging probe with an 8.8-cm inside diameter was used to apply RF pulses to the sample and to receive the NMR signals from the sample.

A dryer with four 660-W heaters and a fan was used to supply air to the probe (Fig. 2). Air temperature was sensed by a thermocouple located near the sample and controlled by a temperature controller. The drying air temperature was 60°C. Air velocity around the sample was 1.83 m/sec. The relative humidity of the drying air was 6%.

The sample was suspended by a plastic sample holder in the center of the imaging probe. Two supports of the sample holder maintained the position of the sample and allowed drying air to pass around it. The longitudinal axis of the ear was parallel to the axis of the probe ($z$ direction, Fig. 2).

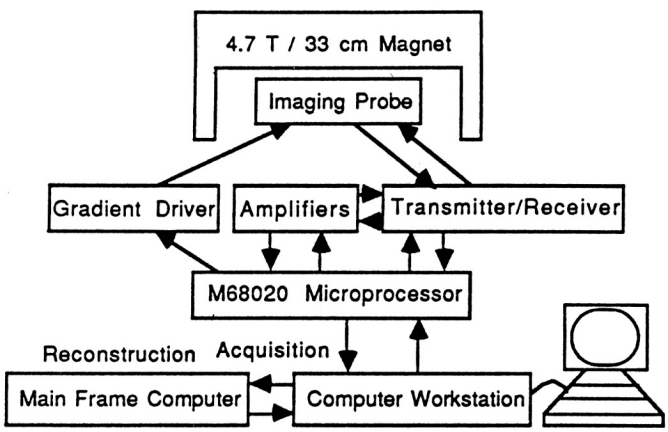


**Fig. 1.** Spectroscopy imaging system: 200-MHz, 300-mm nuclear magnetic resonance imaging system.

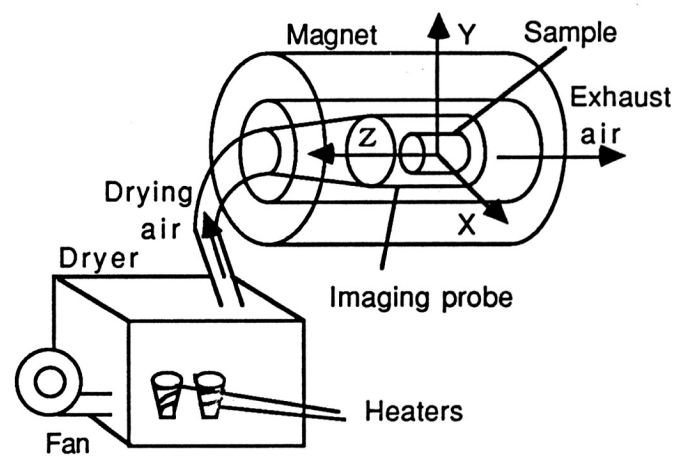


**Fig. 2.** Dryer and system coordinates.

The endosperm and the germ of kernels from the same ear of corn as the test sample were dissected for $T1$ and $T2$ measurements. About 20 g of endosperm and 4 g of germ were measured. The inversion-recovery method (Carr and Purcell 1954) was used for $T1$ measurements and the Hahn spin-echo method (Hahn 1950) for $T2$ measurements. Each measurement was repeated three times, and the mean value was taken as the final result. The measurements were conducted at 60°C (drying temperature) to ensure that the results could be used for data processing. $T1$ values were 1.923 and 0.673 sec for the endosperm and the germ, respectively. $T2$ values were 11 and 8 msec for the endosperm and the germ, respectively. 3-D proton density data were collected by the 3-DFT method. Sixty-four phase encoding steps were used in both the $x$ and $z$ directions (Fig. 2). The increments of the phase encoding gradients were $1.2 \times 10^{-6}$ tesla/cm (T/cm). The readout gradient strength was $1.504 \times 10^{-4}$ T/cm. One set of NMR signals was collected for imaging reconstruction. The total data acquisition time was 68 min.

3-D proton density data for the ear of corn were also collected by the multislice imaging method during drying. Proton density signals from 10 adjacent slices in the $y$-$x$ plane (Fig. 2) were collected. The spin-warp pulse sequence with echo time of $TE = 28$ msec ($\tau = 14$ msec) was used (Edelstein et al 1980). Repetition time $TR$ was set to 10 sec. The gradient strengths were $1.504 \times 10^{-4}$ T/cm in the readout ($y$) direction and $1.7646 \times 10^{-4}$ T/cm in the slice selection ($z$) direction. Slice thickness was 1.294 mm. The increment of the phase encoding gradient was $1.2 \times 10^{-6}$ T/cm. There were 64 phase encoding steps. Each image was reconstructed from one set of NMR signals. The total data acquisition time for each set of multislice data was 10 min 40 sec. Subsequent data were collected every 30 min during a 5-hr drying test. The 3-D images were reconstructed by the Fourier transform method.

To determine the values of moisture profiles from the NMR images, a sample of known moisture content must be measured under the same imaging conditions as used for the test sample. For this purpose, a tube of $CuSO_4$ solution ($1.9541 \times 10^{-3}$ mol/L) was measured with the ear of corn. Since very little $CuSO_4$ was added, the signal intensity from the solution was the same as from pure water. $T1$ and $T2$ of the $CuSO_4$ solution were measured at 60°C. $T1$ was 0.171 sec, and $T2$ was 48 msec ($T1 = 0.073$ sec, and $T2 = 28$ msec at 20°C). The same imaging conditions were used as for the drying tests. The germ contains some oil, which contributes to the NMR signals, but the amount of oil is small compared to the amount of water (4% oil, 50–70% water). Based on this, the proton density profiles were proportionally related to moisture profiles. The values of the $T1$ and $T2$ factors in equation 1 were calculated. By dividing the same values of the factors on both sides of equation 1, the proton density signals for both the corn and the $CuSO_4$ solution were corrected to full signal intensities. The average full intensity of the $CuSO_4$ solution profile was set as 100% moisture content (wb), and therefore the moisture profiles of the corn were scaled proportionally. Since relatively low gradients were used, the diffusion effects on the signal intensity were neglected (expression 2).

Since large repetition times were used ($TR > 5T1$), the influence of $TR$ on signal intensity was negligible (equation 1). The spin-spin relaxation time $T2$ of the endosperm of the corn kernels decreased 2 msec after 5 hr of drying, which caused a decrease of the collected signal intensity. This effect was corrected during the data processing according to equation 1.

Moisture content of the corn kernels was also determined by the oven method at 103°C for 72 hr (ASAE 1989, Standard S352.2). Before the drying test, kernels (50 g) on the same ear of corn as the test section were cut equally into five pieces, dried, and weighed separately. After 5 hr of drying in the NMRI experiment, the endosperms and germs of the corn kernels from the test section were separated. Each endosperm was then cut from the crown to the tip into five equal parts. The germ and endosperm pieces were then placed in small trays and dried with the oven method. The moisture contents of the five parts of the endosperm and the germ were compared with the corresponding moisture contents from the moisture profiles after 5 hr of drying.

## RESULTS AND DISCUSSION

A 3-DFT proton density image of the ear of sweet corn before drying was obtained (Fig. 3), with a spatial resolution of 0.234 mm in each direction. Using a 3-D viewing scheme, the inside structure of the corn ear could be inspected through selected viewing planes. The moisture profiles in any plane could be displayed.

Proton density images of 10 slices of the corn ear during drying were obtained by the multislice method. Figure 4 shows the 2-D multislice images before and after drying. The brightness of the images at a given time is proportional to the moisture content of the corn kernel. Greater intensity was used in Fig. 4 (bottom) than in Fig. 4 (top) to show the structural changes after drying. However, the differences between kernels in each image do not necessarily represent a significant moisture difference between kernels. The brighter images of kernels occur because the slice fully passed through the center of the kernel. The darker images of kernels occur where the slice partially involved the kernel and partially involved the space between adjacent kernels, so the signal intensity was weaker. However, comparisons can be made for the same kernel at different drying times. Shape changes of the kernels were caused by shrinkage and moisture loss during drying. From the same slice image in the two parts of Fig. 4, the moisture loss and shrinkage of the kernels can be found by checking the absolute signal intensities and the structural changes.

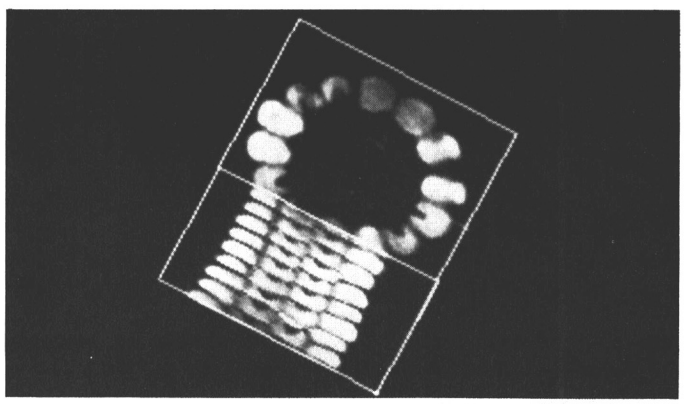

**Fig. 3.** Three-dimensional Fourier transform proton density image of an ear of sweet corn.

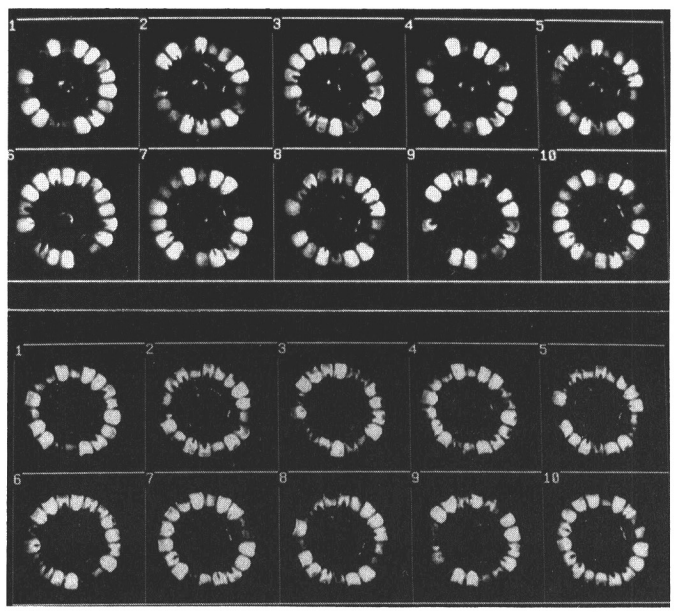


**Fig. 4.** Multislice proton density images of corn. **Top,** before drying; **bottom,** after drying 5 hr.

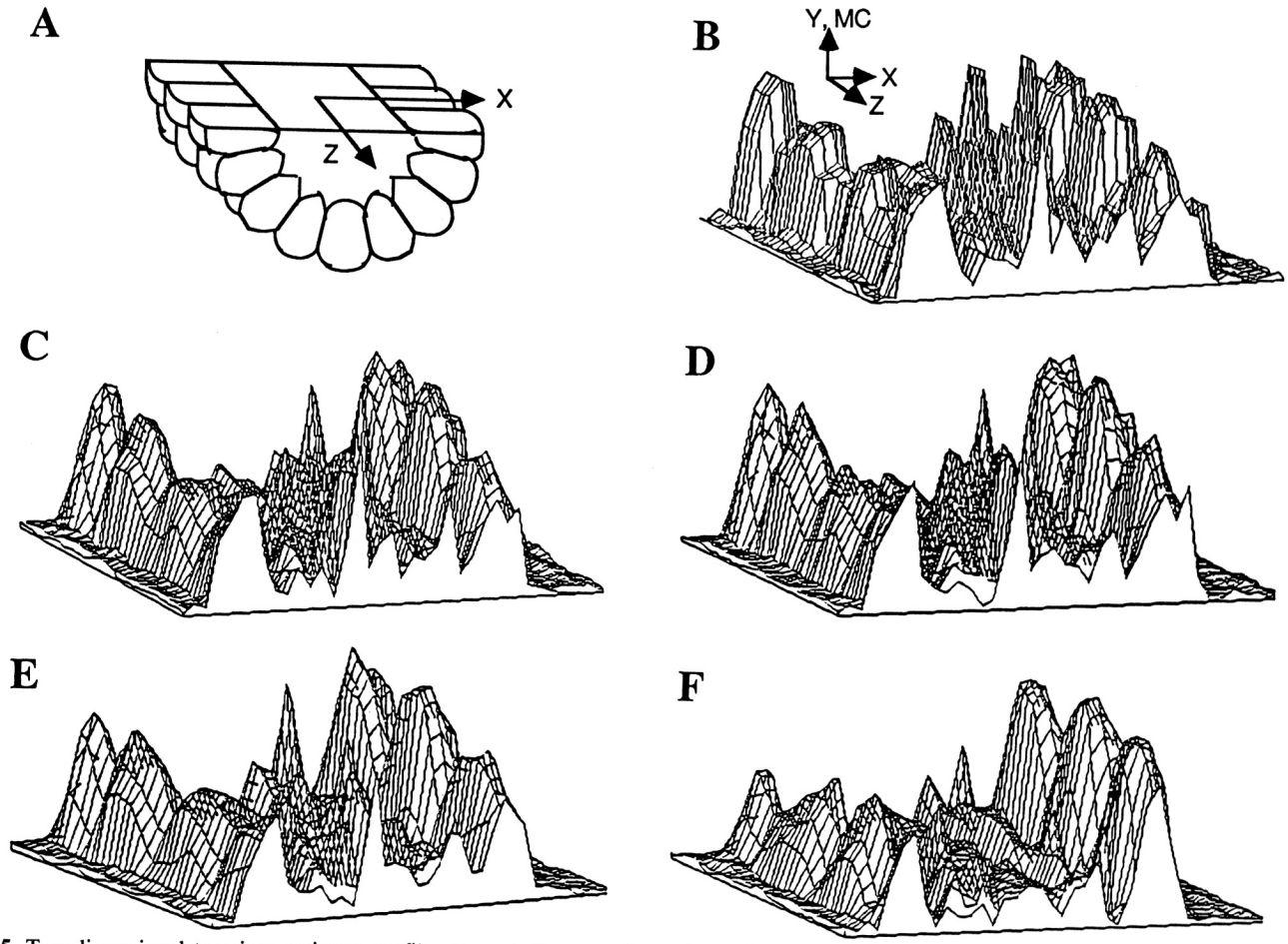


**Fig. 5.** Two-dimensional transient moisture profiles through the central *x-z* plane of an ear of corn. **A,** Viewing plane; **B,** before drying; **C,** after drying 1 hr; **D,** after drying 2 hr; **E,** after drying 3 hr; **F,** after drying 5 hr. MC = moisture content.

From the transient, 3-D proton density images by the multislice method, the 2-D transient moisture profiles from the central *x-z* plane (Fig. 5A) of the corn ear were obtained. Before drying, a moisture gradient existed in the corn kernels (Fig. 5B). After drying started, the moisture content near the crown of the corn kernels decreased more quickly than in the center of the kernels (Fig. 5C).

The surface moisture content of the corn kernels decreased most rapidly as the moisture content of the kernel decreased. The overall shape of the moisture profiles did not change substantially during the drying (Fig. 5C–F). The moisture decreased both in the kernels and in the cob, indicating that the evaporated moisture was supplied by both the kernels and the cob. The shape and magnitude of changes of the 2-D moisture profiles in each individual kernel (Fig. 5) showed that moisture transport occurred in the *x* and *z* directions within individual kernels. For the kernels on the left-hand side of the profile, the nearly identical decrease of moisture content in kernels adjacent to each other indicated that moisture transfer between kernels was not significant. The moisture transfer in the kernels on the right-hand side did not decrease continuously during the drying period. The reasons for this phenomenon were nonuniform drying and movement of the corn since the sample was shrinking during drying.

A single slice was examined in more detail using 2-D enlarged images together with moisture profiles for an axis through the center of the sample (Fig. 6). The height of the profile above the image at each point corresponds to the moisture content at that point on the horizontal axis. The initial moisture distribution in the kernels can be seen from the profile (Fig. 6 left). The moisture content in both kernels and the cob decreased after drying (Fig. 6 right).

Transient moisture profiles during drying were plotted for the images in Fig. 6 (Fig. 7A and B). The overall shapes of the moisture

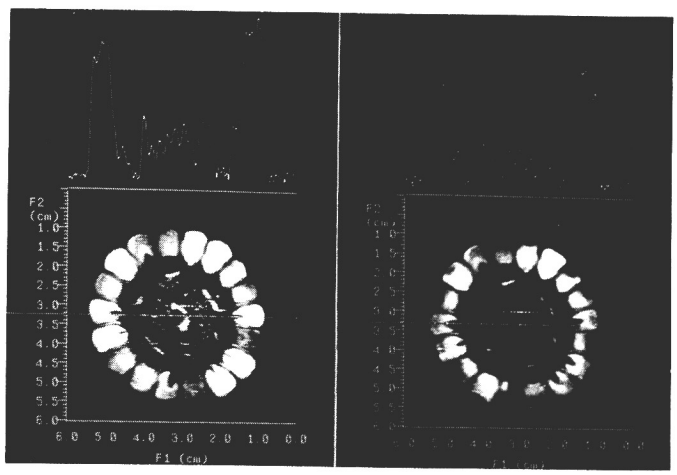


**Fig. 6.** Two-dimensional proton density images and one-dimensional moisture profiles through the center of a single slice of an ear of corn. **Left,** before drying; **right,** after 5 hr of drying.

profiles in the corn kernels were similar throughout the drying process. For the left-most kernel on the horizontal axis in Fig. 6, the drying curves at three different points were plotted (Fig. 8). The curves correspond to points 1.5, 3.5, and 5.0 mm from the crown of the kernel. During the first hour, the 1.5-mm point dried from 70 to 61% (wb); the moisture content at the 3.5-mm point decreased from 79 to 63% (wb); and the moisture content at the 5.0-mm point changed from 78 to 59% (wb). The drying rates decreased throughout the test. For example, the drying rates during the second hour for the same three points were 3.5, 2.6, and 2.0% moisture per hour, respectively. The

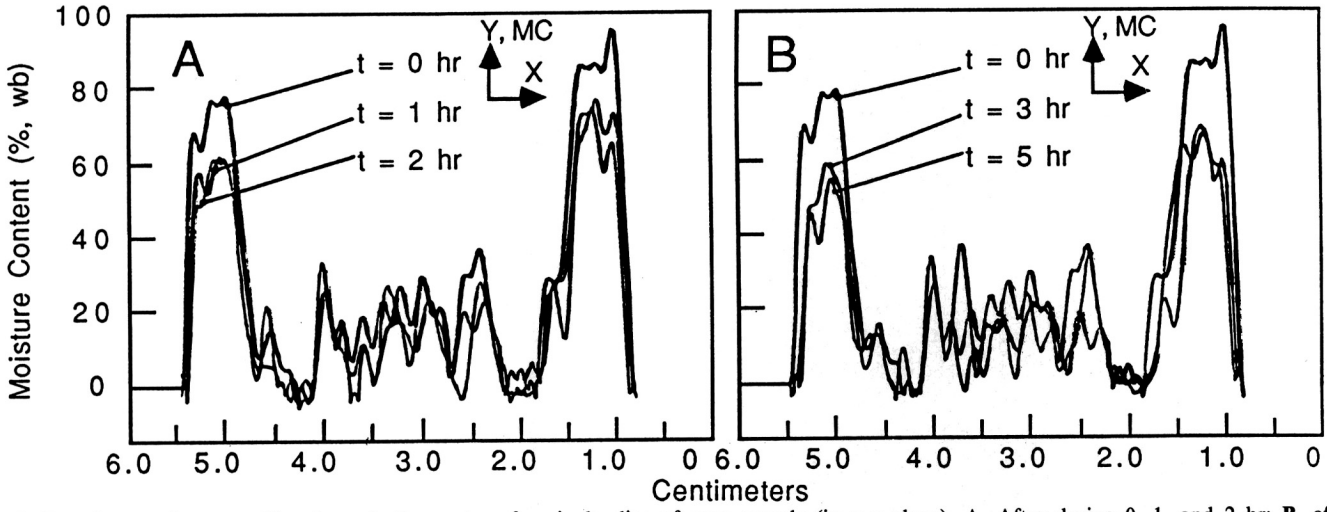


**Fig. 7.** Transient moisture profiles through the center of a single slice of corn sample (in *x-y* plane). **A,** After drying 0, 1, and 2 hr; **B,** after drying 0, 3, and 5 hr. MC = moisture content.

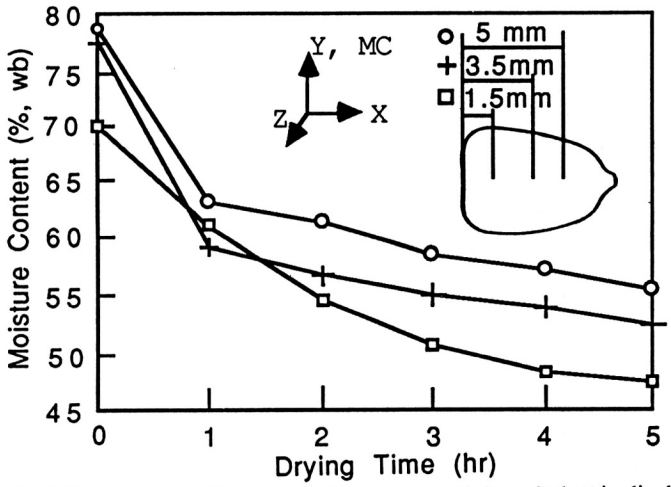


**Fig. 8.** Drying curves of three points in a corn kernel along the longitudinal axis (*z*-direction slice thickness = 1.3 mm). MC = moisture content.

moisture contents obtained from NMRI were within about 10% of those from the oven method. The difference might arise from four sources: 1) slicing of kernels introduces measurement error; 2) *T*2 differences may exist among different parts of the endosperm; 3) the oven drying procedure is for whole kernels; and 4) a random environmental error may occur from the NMRI system. The environmental noise signals resulted in about 3% error in the proton density, compared with the average full signal of the $CuSO_4$ solution. This error was added to the proton density profiles. Since the proton density was proportional to the moisture content, the actual moisture contents were within 3% of the values obtained.

Shrinkage of the corn after 5 hr of drying was measured from the change in the *x* direction (Fig. 7). The shrinkage along the center line was 1.6 mm. The same result was also obtained by physically measuring the corn at that position with a caliper.

## SUMMARY AND CONCLUSIONS

Two methods, 3-DFT and multislice 2-DFT, were used to obtain 3-D proton density images of corn. The shorter data acquisition time of the multislice method was valuable for drying experiments, but the spatial resolution in the slice-selection direction was not as good as with the 3-DFT results.

2-D, transient moisture profiles during drying were obtained from a selected plane of a 3-D image. The profiles were used to analyze moisture transfer and structural changes.

Mass transfer occurred in the *x*- and *z*-directions in individual kernels, but the moisture transfer between kernels during drying was negligible compared with the moisture transfer inside the corn kernels.

Shrinkage of the corn ear during drying was measured from changes of the one-dimensional moisture profiles in a selected direction.

## ACKNOWLEDGMENTS

We acknowledge assistance of the National Science Foundation (CBT-8808748), the Biomedical Magnetic Resonance Laboratory, and the National Center for Supercomputing Applications.

## LITERATURE CITED

AMERICAN SOCIETY OF AGRICULTURAL ENGINEERS. 1989. Moisture measurement—Unground grain and seeds. S352.2. In: ASAE Standards 1989. The Society: St. Joseph, MI.

ANDRIEU, J., and STAMATOPOULOS, A. A. 1986. Moisture and heat transfer modelling during durum wheat pasta drying. Pages 492-498 in: Drying '86, Vol. II. A. S. Mujumdar, ed. Hemisphere Publishing Co., Washington, DC.

CARR, H. Y., and PURCELL, E. M. 1954. Effects of diffusion on free precession in nuclear magnetic resonance experiments. Phys. Rev. 94:630-638.

EDELSTEIN, W. A., HUTCHISON, J. M. S., JOHNSON, G., and REDPATH, T. 1980. Spin warp NMR imaging and applications to human whole-body imaging. Phys. Med. Biol. 25:751.

HAHN, E. L. 1950. Spin echoes. Phys. Rev. 80:580-594.

KUMER, A., WELTI, D., and ERNST, R. R. 1975. NMR Fourier zeugmatography. J. Magn. Reson. 18:69-83.

LAUTERBUR, P. C. 1973. Image formation by induced local interactions: Examples of employing nuclear magnetic resonance. Nature 242:190-191.

LITCHFIELD, J. B., and OKOS, M. R. 1986. Moisture diffusivity in pasta during drying. ASAE Paper 86-6519. American Society of Agricultural Engineers: St. Joseph, MI.

MANSFIELD, P., and MAUDSLEY, A. A. 1976. Planar spin imaging by NMR. J. Phys. C:9 L409-411.

SONG, H., and LITCHFIELD, J. B. 1988. Nondestructive measurement of transient moisture profiles in corn during drying using NMR imaging. ASAE Paper 88-6532. American Society of Agricultural Engineers: St. Joseph, MI.

STARK, D. D., and BRADLEY, W. G., Jr. 1988. Magnetic Resonance Imaging. The C. V. Mosby Co.: St. Louis, MO.

[Received January 8, 1990. Accepted May 25, 1990.]